AGU PUBLICATIONS

Geophysical Research Letters

RESEARCH LETTER
10.1002/2016GL071036

Key Points:
- Mixed-phase clouds occur more commonly than previously believed
- Mixed-phase clouds can be persistent in orographic terrain, like the Alps, under strong orographic forcing
- Regional model simulations are able to simulate mixed-phase clouds and support our observations

Supporting Information:
- Figure S1
- Figure S2
- Figure S3
- Figure S4
- Figure S5
- Supporting Information S1

Correspondence to:
U. Lohmann,
ulrike.lohmann@env.ethz.ch

Citation:
Lohmann, U., J. Henneberger, O. Henneberg, J. P. Fugal, J. Bühl, and Z. A. Kanji (2016), Persistence of orographic mixed-phase clouds, *Geophys. Res. Lett.*, *43*, 10,512–10,519, doi:10.1002/2016GL071036.

Received 2 AUG 2016
Accepted 22 SEP 2016
Accepted article online 24 SEP 2016
Published online 12 OCT 2016

Persistence of orographic mixed-phase clouds

U. Lohmann[1], J. Henneberger[1], O. Henneberg[1], J. P. Fugal[2,3], J. Bühl[4], and Z. A. Kanji[1]

[1]ETH Zurich, Institute of Atmospheric and Climate Science, Zurich, Switzerland, [2]Institute for Atmospheric Physics, Johannes Gutenberg University, Mainz, Germany, [3]Particle Chemistry Department, Max Planck Institute for Chemistry, Mainz, Germany, [4]Leibniz Institute for Tropospheric Research, Leipzig, Germany

Abstract Mixed-phase clouds (MPCs) consist of ice crystals and supercooled water droplets at temperatures between 0 and approximately −38°C. They are thermodynamically unstable because the saturation vapor pressure over ice is lower than that over supercooled liquid water. Nevertheless, long-lived MPCs are ubiquitous in the Arctic. Here we show that persistent MPCs are also frequently found in orographic terrain, especially in the Swiss Alps, when the updraft velocities are high enough to exceed saturation with respect to liquid water allowing simultaneous growth of supercooled liquid droplets and ice crystals. Their existence is characterized by holographic measurements of cloud particles obtained at the high-altitude research station Jungfraujoch during spring 2012 and winter 2013 and simulations with the regional climate model COSMO (Consortium of Small-Scale Modeling).

1. Introduction

The response of clouds to global warming is the most uncertain climate feedback. Uncertainties in cloud processes explain much of the spread in modeled climate sensitivity [*Flato et al.*, 2013]. While most of the spread is related to the uncertainty of the impact of warming on low clouds [*Boucher et al.*, 2013], global climate models traditionally underestimate the coverage of midlevel clouds [*Nam et al.*, 2014]. If clouds with temperatures between 0 and −35°C consist only of supercooled liquid water, they reflect 17 W m^{-2} more radiation back to space as if the same clouds consisted purely of ice [*Lohmann*, 2002]. This is mainly due to the larger sizes of ice crystals causing ice clouds to be optically thinner for the same water content as liquid clouds. In addition, the larger ice crystals sediment more readily, reducing the lifetime and water content of these clouds, and ice crystals have a smaller refractive index than cloud droplets. After accounting for the 5 W m^{-2} smaller longwave cloud radiative effect of pure ice clouds in the MPC regime, the difference in the net cloud radiative effect remains −12 W m^{-2}, demonstrating the necessity to better understand mixed-phase clouds (MPCs). Moreover, a higher fraction of supercooled clouds in the present-day climate implies a higher temperature when CO_2 concentrations are doubled [*Tan et al.*, 2016].

We developed a holographic imager HOLIMO, a cloud particle spectrometer which can distinguish cloud particles according to their shape and thus can differentiate between ice crystals and cloud droplets [*Henneberger et al.*, 2013] down to an equivalent area diameter of about 20 μm (see supporting information and Figure S1). As expected, while the smaller ice crystals are predominantly pristine crystals of various shapes, the larger crystals are more irregular and more aggregated. HOLIMO has been operated successfully to detect MPCs at Jungfraujoch during field campaigns in 2012 [*Henneberger et al.*, 2013]. In order to put the measurements into perspective, we also simulate the observed clouds with the regional model COSMO (Consortium of Small-Scale Modeling).

2. Measurements and Model Simulations

The field measurements were conducted at the Sphinx laboratory (3580 m above sea level) at the high-altitude research station Jungfraujoch, 46°33′N, 7°59′E) in the Bernese Alps, Switzerland. The local orography of the saddle between the Jungfrau peak to the west and the Mönch peak to the east constrains the wind direction at the Sphinx observatory to northwesterly (NW) and southeasterly (SE) winds [*Ketterer et al.*, 2014]. If NW wind conditions at Jungfraujoch are observed, the air masses experience a strong ascent from the Bernese Highlands before arriving at Jungfraujoch, whereas air from the SE experiences a more shallow ascent over the Aletsch glacier (Figure S2). Here we analyze in situ cloud measurements taken during April/May 2012

Table 1. Average Values for the JFJ Measurement Periods[a]

Date	Time	T	u	n	TWC	LWC	IWC	N_i	z_B	dd	Cloud Type
SE wind cases:		−9.5	6.8	558	64	57	7	39			
3/4/12	15:23–22:27	−9.3	7.8	38	83	82	2	5	79	SW	thin Cu
4/4/12	08:00–24:00	−7.9	10.5	192	48	45	2	13	44	SW	thin St/some Cu
5/4/12	05:05–20:10	−7.7	1.5	213	87	82	5	28	78	S	thin Cu then St
14–15/4/12	20:50–01:10	−11.1	6.1	51	87	77	10	56	90	SE	St
15/4/12	10:15–13:45	−6.0	3.1	26	72	67	6	3	61	–	St
18/4/12	09:30–16:40	−8.7	4.0	74	101	77	23	130	94	SW	young St
1/5/12	13:30–15:30	−4.8	8.7	19	27	26	1	7	22	S	thin St
11/2/13	14:50–18:00	−20.3	7.9	59	25	2	24	90	42	S	thick St
NW wind cases:		−17.2	8.0	1476	192	73	119	550			
6–7/4/12	20:50–07:14	−9.5	3.4	170	150	126	24	60	143	W	Cu
29/1/13	06:57–08:40	−8.0	12.2	43	58	37	22	90	53	NW	St
4/2/13	10:00–19:35	−12.1	12.4	166	144	70	74	470	153	W	first St then Cu
5/2/13	13:30–17:40	−16.7	12.8	132	130	2	127	470	171	NW	thick St
6/2/13	09:30–23:50	−20.4	7.2	200	221	18	202	750	339	NW	thick St
7/2/13	09:15–22:20	−24.5	8.8	321	218	74	174	1010	417	NW	first thin St then Cu
8/2/13	09:07–10:05	−25.4	4.6	34	253	76	177	730	499	NW	thin St
12/2/13	12:12–22:00	−19.3	7.7	254	239	123	116	450	345	NW	thin St
14/2/13	20:00–21:50	−13.8	8.6	42	264	54	210	830	293	W	first St then Cu

[a]The variable n denotes the number of intervals and dd the synoptic wind direction. Date is formatted as day/month/year, time is given in UTC, temperature T in °C, wind speed u in m s^{-1}, TWC, LWC, and IWC in mg m^{-3}, N_i in L^{-1}, and height above cloud base z_B in m. Cloud types are identified from satellite images.

and January/February 2013. In total, 2034 100 s intervals (56.5 h) of cloud observations with HOLIMO were analyzed covering a temperature range between −5 and −25°C on 17 different days, eight of which had air arriving from SE and nine from NW directions. We choose to define MPCs as those clouds in which the ratio of the ice water content (IWC) to the total water content (TWC, being the sum of the liquid and ice water content) is between 10 and 90%, consistent with the definition in *Korolev et al.* [2003].

The cloud particle data were measured by our self-developed holographic imager HOLIMO II [*Henneberger et al.*, 2013] (Supporting Information S1). Cloud particles from 6 μm to 250 μm were analyzed using a shape-based algorithm to classify particles into liquid droplets or ice crystals [*Fugal and Shaw*, 2009]. The minimum size for an ice crystal was set to 20 μm, which is 7 times the pixel pitch or 6 times the smallest detectable feature [*Henneberger et al.*, 2013]. The mass-dimension relation from *Cotton et al.* [2013] was used to estimate the ice water content. For the ambient wind direction, horizontal wind speed and air temperature data of the MeteoSwiss station at Jungfraujoch were available. An overview over all cloud cases is given in Table 1 and with standard deviations in Table S1.

For simulations, the regional weather and climate model COSMO [*Baldauf et al.*, 2011] was used with a horizontal resolution of 1 km (0.01° × 0.01°), 60 vertical hybrid levels and a temporal resolution of 10 s. With 96 × 100 grid points a region of roughly 96 × 100 km is covered with Jungfraujoch located in the center of the model domain. Through smoothing of orography, the height of the Jungfraujoch is reduced to 3226 m. The simulations are driven by hourly 2.2 km × 2.2 km analysis data from MeteoSwiss. Cloud microphysics are represented by a two-moment microphysics scheme [*Seifert and Beheng*, 2006] considering six hydrometeor classes (cloud droplets, ice crystals, raindrops, snowflakes, graupel, and hail particles). COSMO has previously been used to study the impact of ice nucleating particles (INP) on the development of precipitation in idealized orographic MPCs [*Muhlbauer and Lohmann*, 2009]. Here it will be used with real topography but a simplified treatment of INP, where heterogeneous ice nucleation is parameterized using a constant aerosol number concentration for different aerosol types such as dust, soot, and organics. The fraction of aerosol particles that act as INP is prescribed as a function of temperature and supersaturation for each type [*Phillips et al.*, 2008].

The concentration of cloud condensation nuclei (CCN) is also prescribed in this version of COSMO. Constant number concentrations imply that the CCN and INP concentrations are replenished every time step, which is not realistic but provides an upper limit on their concentrations. Future aerosol-cloud studies with COSMO will be carried out with an aerosol module coupled to COSMO.

3. Results

Observations of frontal clouds obtained in situ from aircraft measurements over Canada [*Korolev et al.*, 2003] show that clouds between 0 and −35°C are predominantly either supercooled liquid or ice, but only 20% of them are mixed-phase almost irrespective of the temperature (Figure 1). A low percentage of MPCs is expected due to their thermodynamic instability resulting from the difference in the saturation vapor pressure over liquid water and over ice. Once ice crystals form in a cloud of supercooled water droplets, they rapidly grow to precipitation size because their environment is supersaturated with respect to ice. In a MPC, once the relative humidity drops below saturation with respect to water, ice crystals will grow at the expense of their neighboring evaporating cloud droplets. This process is known as the Wegener-Bergeron-Findeisen process [*Wegener*, 1911] and can result in a glaciated cloud. Alternatively, if only a few ice crystals nucleate and grow sufficiently large, they will sediment leaving behind (partially evaporated) cloud droplets. In summary, in order to sustain MPCs, supersaturation with respect to water is needed to activate new aerosol particles into cloud droplets and to allow condensational growth of droplets and thus to counteract the sinks of cloud droplets due to freezing, riming, and the Wegener-Bergeron-Findeisen process.

MPCs in Israel [*Borovikov et al.*, 1963] are more common than over Canada [*Korolev et al.*, 2003] with a maximum of 60% in the temperature range between −10 and −15°C, where the difference in vapor pressure over water and ice is largest and the Wegener-Bergeron-Findeisen process would be strongest. MPCs in this temperature range are rare at the Jungfraujoch if the air masses approach the Jungfraujoch from the SE with a shallow ascent (Figure 1), but occur in over 75% of the time in NW wind cases with strong uplifts. The frequency of occurrence of MPCs increases with decreasing temperature and peaks with more than 90% at the coldest temperatures we measured between −20 and −25°C. *Bühl et al.* [2013] investigated MPCs in terms of primary ice formation with a combination of lidar and radar over Leipzig. The definition of liquid and MPCs varies from that in this study in that clouds in which ice formation is detected are mixed-phase, all other clouds with no ice formation and only a stable liquid layer are liquid clouds. The fraction of liquid and MPCs agrees well with the Jungfraujoch measurements at the warmer temperatures (Figure 1). Because pure ice clouds were not investigated over Leipzig, the fraction of MPCs has to be regarded with caution at colder temperatures.

We calculated glaciation times for zero updraft velocity according to *Korolev and Isaac* [2003]. It depends on the ice particle number concentration N_i, liquid and ice water content next to a weak dependency on temperature and pressure. According to these calculations our observed MPCs at Jungfraujoch should survive less than 1 h (Figure 2). In the presence of an updraft, glaciation times can be much higher as is evident from our observations that show the persistence of orographic MPCs of up to 8 h under certain circumstances (Figure S3).

What causes the persistent MPCs for NW wind cases with strong uplifts? Five different possibilities are discussed: (1) Are these MPCs caused by differences in updraft velocities due to the different slopes of the orography between the NW and SE wind cases (Figure S2)? (2) Are the number concentrations of CCN and/or INP different between the NW and SE wind cases? (3) What is the role of secondary ice multiplication and of other ice sources like blowing snow and hoarfrost from the surface or of ice crystals sedimenting from above? (4) Is the height above cloud base at which we measure the cloud age or the cloud thickness different between NW and SE wind conditions? (5) Do we have systematic measurement errors and what are the limitations of distinguishing between ice crystals and cloud droplets only above 20 μm?

No reliable measurements of the updraft velocity are available at Jungfraujoch. Even if they were, they may not be representative for the conditions at cloud base, because cloud base estimated from the liquid water content and assuming adiabatic ascent is several hundred meters below the Jungfraujoch. *Hammer et al.* [2015] tried to infer updraft velocities at Jungfraujoch from horizontal wind measurements, but this method is rather uncertain. In addition, the mean horizontal velocity of the NW cases of 8 ± 3.7 m s^{-1} is not significantly larger than in the SE cases of 6.8 ± 3.6 m s^{-1}. Therefore, we instead decided to simulate the periods of the measurement campaigns using the regional model COSMO. We stratified the frequency of occurrence of vertical velocity in COSMO for all observed cloud cases into no clouds, liquid, mixed-phase, and ice clouds up to the

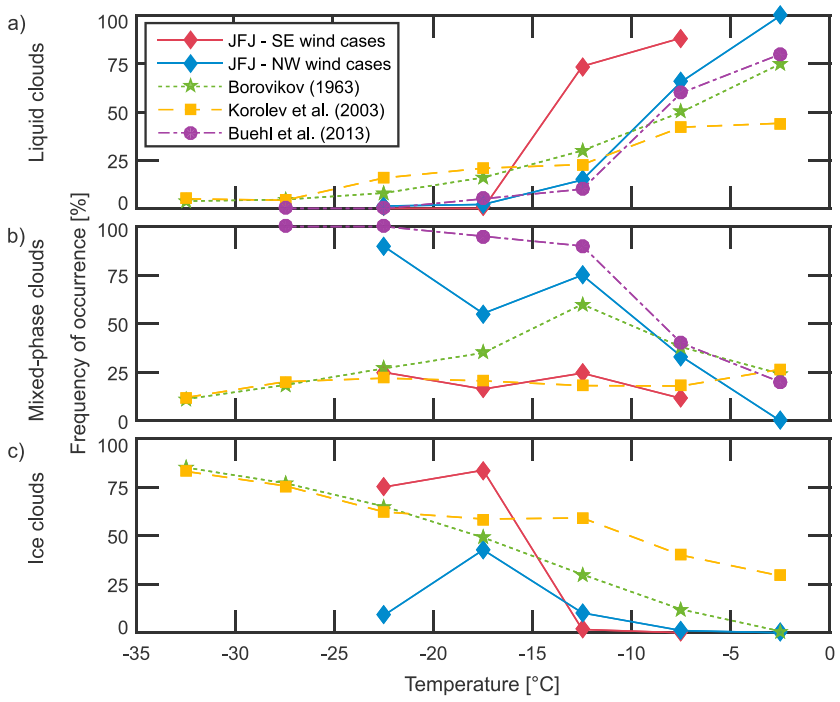

Figure 1. Percentage of (a) liquid water, (b) mixed-phase, and (c) ice clouds between −35 and 0°C as composed from three different studies: Frontal clouds over Canada (updated from *Korolev et al.* [2003]), various clouds over Israel [*Borovikov et al.*, 1963] and Leipzig [*Bühl et al.*, 2013], and orographic clouds obtained at Jungfraujoch summarized in Table 1.

altitude of the Jungfraujoch (Figure 3). For NW wind cases, the simulated vertical velocities range between 0 and 4 m s^{-1} and thus are considerably higher than for SE wind cases, where wind speeds between −1.3 and 0.5 m s^{-1} were simulated.

The vertical velocities are smallest in cloud-free conditions, followed by pure ice clouds, MPCs, and liquid clouds. Higher vertical velocities cause a faster adiabatic expansion and cooling of the air mass resulting in higher supersaturations. Because the saturation vapor pressure over supercooled water is higher than over ice, higher updraft velocities are expected and simulated in clouds containing cloud droplets (liquid clouds and MPCs) than in pure ice clouds as shown in Figure 3. The considerable overlap of the frequency of

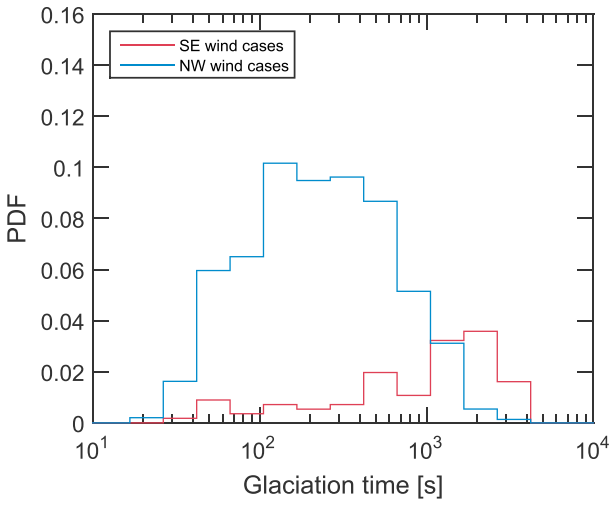

Figure 2. Probability density function normalized to the total number of SE, respectively NW wind cases of the calculated glaciation time assuming zero vertical velocity [*Korolev and Field*, 2008] for our observed cloud cases.

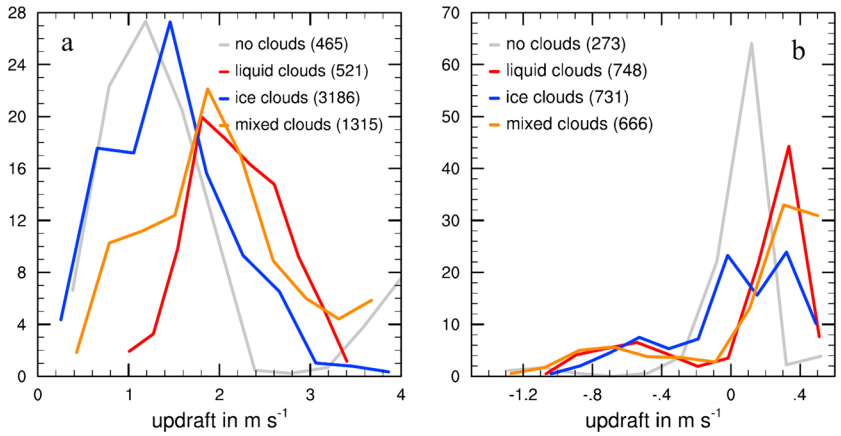

Figure 3. Histogram of the frequency of occurrence of vertical wind velocity (m s^{-1}) for cloud-free, liquid, mixed-phase, and ice clouds aggregated at all altitudes between the surface (between 2897 and 3226 m) and 3550 m as obtained from simulations with the COSMO model for all observed (left) NW wind cases and (right) SE wind cases.

occurrence histograms of vertical velocity is mostly due to the large variability between different cloud conditions such as cloud base, cloud age, initial CCN and INP concentrations, and dynamics. According to COSMO simulations, MPCs can on the one hand form from a fully glaciated cloud when locally the updraft velocity exceeds that required for saturation with respect to water as simulated for the NW case on 14 February 2013 (not shown). On the other hand, cloud cases exist where the cloud mainly consists of supercooled water, primary ice is formed only locally close to the Jungfraujoch, and the cloud is just beginning the process of glaciating.

The number concentrations of CCN and INP observed at Jungfraujoch are not statistically different between NW and SE wind conditions [*Boose et al.*, 2016] and thus cannot explain the differences in the occurrence of MPCs. The number concentration of INP is orders of magnitude smaller than the observed N_i suggesting that secondary or other ice production mechanisms took place after the first ice crystals were formed. If ice nucleation took place upwind of the Jungfraujoch, then the INP concentrations observed at Jungfraujoch would not be responsible for the observed N_i. The scarcity of INP may, however, be responsible for the large fraction of supercooled liquid water clouds that are found between −15 to −10°C in SE wind conditions (Figure S4).

Secondary ice production mechanisms that could have operated between the primary ice nucleation events and when the cloud arrived at Jungfraujoch include the Hallett-Mossop process [*Hallett and Mossop*, 1974] in the regions of the cloud where the criteria for its occurrence are met (temperatures between −3 and −8°C in the presence of supercooled cloud droplets larger than 25 μm in diameter and graupel particles larger than 0.5 mm in diameter). Secondary ice production was probably larger during NW wind cases with strong uplifts, where N_i is an order of magnitude larger than that during SE wind cases (Table 1).

In addition, surface-based processes probably caused or at least contributed to the observed ice crystals at the warmest subzero temperatures, especially to the higher N_i during NW cases, such as hoar frost crystals generated where the cloud encounters the snow surface [*Farrington et al.*, 2015] and at higher wind speeds also blowing snow [*Lloyd et al.*, 2015]. According to our holographic measurements, fragments of snow flakes are rare during all conditions. Most importantly, the difference between NW and SE wind cases arises because of the presence of the liquid phase during NW cases, which surface-based sources of ice crystals cannot explain.

We did not have a ceilometer available during these measurements, and therefore, we do not know the vertical extent of the cloud. Thus, ice crystals could have formed in colder regions higher up in the cloud and sedimented causing the cloud to glaciate by riming and the Wegener-Bergeron-Findeisen process. This might indeed be the case for the glaciated clouds observed during SE wind conditions where updraft velocities are generally lower than the fall velocity of ice particles as supported by our model simulations (Figure S5a). On the contrary, this cannot explain the NW wind cases where the simulated updraft velocities are generally larger than the fall velocity of ice particles (Figure S5b). These higher vertical velocities will prevent ice crystals from falling through the lower parts of the clouds and explain why the liquid water is not depleted.

Because we do not have cloud base measurements for our cloud events, we estimated cloud base assuming an adiabatic liquid water content with the average temperatures and pressures of each day of the measurement campaigns. These estimates yield that Jungfraujoch is between 20 and 500 m above cloud base. Cloud base height is on average 60 m below the Jungfraujoch for SE wind cases and 270 m for NW wind cases. If significant entrainment took place or if the cloud precipitates, then cloud base would be lower. Being closer to cloud base and observing generally warmer temperatures for clouds from SE with shallow ascent explains the generally smaller IWC/TWC ratios (Figure S4) but not the absence of intermediate IWC/TWC ratios. At 270 m above cloud base (for the NW cases), one could expect a higher frequency of fully glaciated clouds. This, in general, is not the case. There are only two almost fully glaciated cloud cases in the data set, one during SE wind conditions and one during NW wind conditions, both at the intermediate temperatures between −15 and −20°C (Figure S4) and with intermediate heights above cloud base of 40 m for the SE case and 170 m for the NW case.

In the absence of ceilometer data we cannot estimate the cloud thickness. Therefore, we analyzed our data in terms of cloud type from satellite data (Table 1). It shows that our observed clouds were predominantly nonprecipitating stratus clouds. Some of the supercooled liquid water SE wind cases may be similar to the Arctic and midlatitude midlevel MPC cases, in which ice particle sedimentation readily removes the newly formed ice particles from the cloud without depleting the liquid water.

Small ice crystals below 30 μm with nearly circular shadowgraphs might be misclassified as spherical cloud droplets. As the cloud droplet concentrations N_d generally are much higher than N_i, the missed ice crystals would not significantly change the liquid cloud properties but can contribute significantly to the total N_i. N_i with sizes >250 μm, our upper limit of measurements, decrease exponentially [*Lloyd et al.*, 2015]. They could contribute significantly to the ice water content, which would shift the IWC/TWC ratio to higher values. Nevertheless, these larger ice crystals are likely too few to noticeably change the evolution of the cloud.

4. Conclusions

We showed that MPCs are frequently found in the Swiss Alps, when the updraft velocities are high enough to exceed saturation with respect to liquid water allowing simultaneous growth of supercooled liquid droplets and ice crystals. Most of the time, the observed N_i were not sufficiently high to convert these MPCs into a fully glaciated cloud. We calculated that ice crystals forming at water saturation and growing by diffusion at a zero updraft velocity need between 10 to 15 min to reach our average observed size of 80 μm at the observed temperatures, which is longer than the majority of the estimated glaciation times for strong uplifts (NW wind cases; Figure 2). Here ice crystal sedimentation from upper levels should be small because these ice crystals should be smaller than our average size of 80 μm and have fall velocities of less than 1 m s^{-1} [*Mitchell*, 1996], which is less than most of the simulated updraft velocities for MPCs for these cases. It is possible that the steep orography on the NW side of Jungfraujoch causes turbulence and high updraft velocities in pockets of the cloud where the hydrometeor concentration is so small that new cloud droplets are activated. We will investigate this possibility in future research.

In the Arctic [*Morrison et al.*, 2012] and in midlevel layer clouds over Leipzig [*Bühl et al.*, 2016], a supercooled liquid water layer is frequently found on top of the MPC. It is formed there because radiative cooling and the associated turbulence create supersaturation with respect to water. Ice crystals that form in this layer grow rapidly to large sizes and sediment. These MPC layers seem to be stable as long as the ice water fractions remain below 10% according to the observations over Leipzig [*Bühl et al.*, 2016]. These findings correspond to our SE wind cases which have comparable updraft velocities as the clouds over Leipzig and are predominantly either supercooled clouds or ice clouds (Figure S4).

For orographic clouds, two different regimes can be distinguished depending on the steepness of the orography (Figures 4 and S2): First, there is a microphysics regime associated with weak updrafts and small supersaturations (Figure 3) as also observed over Leipzig and in the Arctic. Here ice particles grow by diffusion due to the Wegener-Bergeron-Findeisen process, and the physical and chemical properties of the aerosol particles matter more for the cloud evolution. Second, there is a dynamics regime where strong updrafts stabilize the MPC by activation of more and smaller aerosol particles and growth of existing cloud droplets. The associated stronger turbulence might also enhance growth of ice crystals by aggregation and secondary ice production due to collisional breakup and uplift of ice particles from the surface. However, the higher vertical

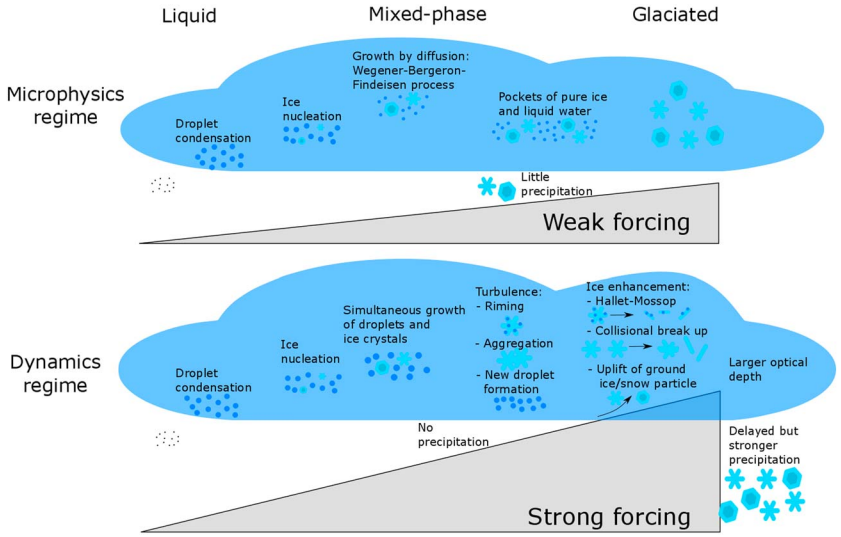

Figure 4. Schematic of the processes in orographic clouds transitioning from the liquid over the mixed-phase to the glaciated state in case of a (top) weak orographic forcing and (bottom) strong orographic forcing.

velocities in these clouds prevent the ice crystals from falling through the regions of supercooled liquid water and thus prevent the cloud from glaciating.

Our findings imply that cloudy regions with stronger updrafts are more prone to prolonged MPC conditions and aircraft icing. For climate modeling, more persistent MPCs than glaciated clouds mean that the optical depths of these clouds is higher and that the climate sensitivity in a $2xCO_2$ climate will be larger because the negative cloud phase feedback (conversion from ice to liquid due to the higher temperatures) is smaller [*Tan et al.*, 2016].

Acknowledgments
We like to acknowledge financial support from the MeteoSwiss GAW project and the EU FP7 project BACCHUS under grant agreement no. 603445. Thank you to Hannes Wydler and the Custodians at the Jungfraujoch (Maria and Urs Ortz and Joan and Martin Fischer) for their help with the field measurements and MeteoSwiss for providing the hourly analysis data and measurements of wind direction and temperature. The data used are listed in the references and can be found here: https://polybox.ethz.ch/index.php/s/UJFdrzP7DqcmhI0.

References

Baldauf, M., A. Seifert, J. Foerstner, D. Majewski, M. Raschendorfer, and T. Reinhardt (2011), Operational Convective-Scale Numerical Weather Prediction with the COSMO Model: Description and Sensitivities, *Mon. Weather Rev.*, *139*(12), 3887–3905, doi:10.1175/MWR-D-10-05013.1.

Boose, Y., et al. (2016), Ice nucleating particle measurements at 241 K during winter months at 3580 m a.s.l. in the Swiss Alps, *J. Atmos. Sci.*, *73*, 2203–2228, doi:10.1175/JAS-D-15-0236.1.

Borovikov, A. M., I. I. Gaivoronskii, E. G. Zak, V. V. Kostarev, I. P. Mazin, V. E. Minervin, A. K. Khrgian, and S. M. Shmeter (1963), *Cloud Physics*, Israel Program for Sci. Transl., Jerusalem.

Boucher, O., et al. (2013), Clouds and aerosols, in *Climate Change 2013: The Physical Science Basis. Contribution of Working Group I to the Fifth Assessment Report of the Intergovernmental Panel on Climate Change*, edited by T. Stocker et al., pp. 571–657, Cambridge Univ. Press, Cambridge, U. K. and New York.

Bühl, J., A. Ansmann, P. Seifert, H. Baars, and R. Engelmann (2013), Toward a quantitative characterization of heterogeneous ice formation with lidar/radar: Comparison of CALIPSO/CloudSat with ground-based observations, *Geophys. Res. Lett.*, *40*, 4404–4408, doi:10.1002/grl.50792.

Bühl, J., P. Seifert, A. Myagkov, and A. Ansmann (2016), Relation between ice and liquid water mass in mixed-phase cloud layers measured with Cloudnet, *Atmos. Chem. Phys. Discuss.*, *2016*, 1–19, doi:10.5194/acp-2016-25.

Cotton, R. J., P. R. Field, Z. Ulanowski, P. H. Kaye, E. Hirst, R. S. Greenaway, I. Crawford, J. Crosier, and J. Dorsey (2013), The effective density of small ice particles obtained from in situ aircraft observations of mid-latitude cirrus, *Q. J. R. Meteorol. Soc.*, *139*(676), 1923–1934, doi:10.1002/qj.2058.

Farrington, R. J., P. J. Connolly, G. Lloyd, K. N. Bower, M. J. Flynn, M. W. Gallagher, P. R. Field, C. Dearden, and T. W. Choularton (2015), Comparing model and measured ice crystal concentrations in orographic clouds during the INUPIAQ campaign, *Atmos. Chem. Phys. Discuss.*, *15*(18), 25,647–25,694, doi:10.5194/acpd-15-25647-2015.

Flato, G., et al. (2013), Evaluation of climate models, in *Climate Change 2013: The Physical Science Basis. Contribution of Working Group I to the Fifth Assessment Report of the Intergovernmental Panel on Climate Change*, edited by T. Stocker et al., pp. 741–866, Cambridge Univ. Press, Cambridge, U. K. and New York.

Fugal, J. P., and R. A. Shaw (2009), Cloud particle size distributions measured with an airborne digital in-line holographic instrument, *Atmos. Meas. Tech.*, *2*(1), 259–271, doi:10.5194/amt-2-259-2009.

Hallett, J., and S. C. Mossop (1974), Production of secondary ice particles during riming process, *Bull. Am. Meteorol. Soc.*, *55*, 679–679.

Hammer, E., N. Bukowiecki, B. P. Luo, U. Lohmann, C. Marcolli, E. Weingartner, U. Baltensperger, and C. R. Hoyle (2015), Sensitivity estimations for cloud droplet formation in the vicinity of the high-alpine research station Jungfraujoch (3580 m a.s.l.), *Atmos. Chem. Phys.*, *15*(18), 10,309–10,323, doi:10.5194/acp-15-10309-2015.

Henneberger, J., J. P. Fugal, O. Stetzer, and U. Lohmann (2013), HOLIMO II: A digital holographic instrument for ground-based in situ observations of microphysical properties of mixed-phase clouds, *Atmos. Meas. Tech.*, *6*, 2975–2987, doi:10.5194/amt-6-2975-2013.

Ketterer, C., P. Zieger, N. Bukowiecki, M. Collaud Coen, O. Maier, D. Ruffieux, and E. Weingartner (2014), Investigation of the planetary boundary layer in the Swiss Alps using remote sensing and in situ measurements, *Boundary Layer Meteorol.*, *151*(2), 317–334, doi:10.1007/s10546-013-9897-8.

Korolev, A., and P. R. Field (2008), The effect of dynamics on mixed-phase clouds: Theoretical considerations, *J. Atmos. Sci.*, *65*(1), 66–86, doi:10.1175/2007jas2355.1.

Korolev, A. V., and G. A. Isaac (2003), Phase transformation of mixed-phase clouds, *Q. J. R. Meteorol. Soc.*, *129*, 19–38.

Korolev, A. V., G. A. Isaac, S. G. Cober, W. Strapp, and J. Hallett (2003), Microphysical characterization of mixed-phase clouds, *Q. J. R. Meteorol. Soc.*, *129*, 39–65.

Lloyd, G., et al. (2015), The origins of ice crystals measured in mixed-phase clouds at the high-alpine site Jungfraujoch, *Atmos. Chem. Phys.*, *15*(22), 12,953–12,969, doi:10.5194/acp-15-12953-2015.

Lohmann, U. (2002), Possible aerosol effects on ice clouds via contact nucleation, *J. Atmos. Sci.*, *59*, 647–656.

Mitchell, D. L. (1996), Use of mass- and area-dimensional power laws for determining precipitation particle terminal velocities, *J. Atmos. Sci.*, *53*(12), 1710–1723, doi:10.1175/1520-0469(1996)053<1710:UOMAAD>2.0.CO;2.

Morrison, H., G. de Boer, G. Feingold, J. Harrington, M. D. Shupe, and K. Sulia (2012), Resilience of persistent Arctic mixed-phase clouds, *Nat. Geosci.*, *5*(1), 11–17.

Muhlbauer, A., and U. Lohmann (2009), Sensitivity studies of aerosol-cloud interactions in mixed-phase orographic precipitation, *J. Atmos. Sci.*, *66*(9), 2517–2538, doi:10.1175/2009JAS3001.1.

Nam, C. C. W., J. Quaas, R. Neggers, C. Siegenthaler-Le Drian, and F. Isotta (2014), Evaluation of boundary layer cloud parameterizations in the ECHAM5 general circulation model using CALIPSO and CloudSat satellite data, *J. Adv. Model. Earth Syst.*, *6*, 300–314, doi:10.1002/2013MS000277.

Phillips, V. T. J., P. J. DeMott, and C. Andronache (2008), An empirical parameterization of heterogeneous ice nucleation for multiple chemical species of aerosol, *J. Atmos. Sci.*, *65*, 2757–2783.

Seifert, A., and K. D. Beheng (2006), A two-moment cloud microphysics parameterization for mixed-phase clouds. Part 1: Model description, *Meteorol. Atmos. Phys.*, *92*, 45–66.

Tan, I., T. Storelvmo, and M. D. Zelinka (2016), Observational constraints on mixed-phase clouds imply higher climate sensitivity, *Science*, *352*(6282), 224–227, doi:10.1126/science.aad5300.

Wegener, A. (1911), *Thermodynamik der Atmosphäre*, Barth, Leipzig, Germany.